Research Paper https://doi.org/10.7733/jnfcwt.2023.033

Characterization of the Purified Ca-type Bentonil-WRK Montmorillonite and Its Sorption Thermodynamics With Cs(I) and Sr(II)

Seonggyu Choi*, Bong-Ju Kim, Surin Seo, Jae-Kwang Lee, and Jang-Soon Kwon
Korea Atomic Energy Research Institute, 111, Daedeok-daero 989beon-gil, Yuseong-gu, Daejeon 34057, Republic of Korea

(Received August 25, 2023 / Revised September 7, 2023 / Approved September 11, 2023)

Thermodynamic sorption modeling can enhance confidence in assessing and demonstrating the radionuclide sorption phenomena onto various mineral adsorbents. In this work, Ca-montmorillonite was successfully purified from Bentonil-WRK bentonite by performing the sequential physical and chemical treatments, and its geochemical properties were characterized using X-ray diffraction, Brunauer-Emmett-Teller analysis, cesium-saturation method, and controlled continuous acid-base titration. Further, batch experiments were conducted to evaluate the adsorption properties of Cs(I) and Sr(II) onto the homoionic Ca-montmorillonite under ambient conditions, and the diffuse double layer model-based inverse analysis of sorption data was performed to establish the relevant surface reaction models and obtain corresponding thermodynamic constants. Two types of surface reactions were identified as responsible for the sorption of Cs(I) and Sr(II) onto Ca-montmorillonite: cation exchange at interlayer site and complexation with edge silanol functionality. The thermodynamic sorption modeling provides acceptable representations of the experimental data, and the species distributions calculated using the resulting reaction constants accounts for the predominance of cation exchange mechanism of Cs(I) and Sr(II) under the ambient aqueous conditions. The surface complexation of cationic fission products with silanol group slightly facilitates their sorption at pH > 8.

Keywords: Thermodynamic sorption modeling, Bentonil-WRK montmorillonite, Cesium, Strontium, Cation exchange, Surface complexation

*Corresponding Author.
Seonggyu Choi, Korea Atomic Energy Research Institute, E-mail: schoi21@kaeri.re.kr, Tel: +82-42-866-6459

ORCID

Seonggyu Choi	http://orcid.org/0000-0002-5784-5034	Bong-Ju Kim	http://orcid.org/0000-0001-9934-8899
Surin Seo	http://orcid.org/0009-0009-9358-1679	Jae-Kwang Lee	http://orcid.org/0000-0003-3903-0904
Jang-Soon Kwon	http://orcid.org/0000-0002-1826-6443		

1. Introduction

Safe disposal of high-level radioactive waste (HLW), including the discharged spent nuclear fuel (SNF) and contaminated by-products generated from the ensuing chemical treatments, has become a serious issue in many countries operating the nuclear power plants. Among the various concepts of radioactive waste management proposed thus far, deep geological disposal (DGD) has been considered as the most proven technology and widely agreed upon as the safest solution for the permanent isolation of HLW from the biosphere. The DGD system consists of multiple components; from a hydrogeochemical perspective, the bentonite clay-based engineered barriers are designed to perform the primary functions of 1) preventing the inflow of groundwater and any reactive substances that could compromise the safety of waste canister and 2) retarding the migration of released radionuclides into geosphere by providing sufficient chemical sorption capacity [1]. Thus far, the sorption behaviors of dissolved chemical species onto mineral adsorbents have been widely described and quantified using the concept of sorption-desorption distribution coefficient (Kd), which is simply defined as a ratio of species concentration in adsorbent to that in supernatant phases; since any specific reaction mechanisms are not considered and reflected in the Kd concept, an experimental Kd value is intrinsically dependent on the geochemical conditions (e.g., pH, Eh, S/L, and etc.) under which it was evaluated. In this framework, substantial scientific efforts have been made to develop a robust basis for parameterizing the sorption phenomena more reliably, and the application of thermodynamic sorption modeling (TSM) [2-4], which is based on the conventional chemical principle of mass action laws (MALs), has been actively studied to enhance the overall predictability on migration of radionuclides under a wide range of geochemical conditions.

Montmorillonite, which is a 2:1 phyllosilicate belonging to smectite group, constitutes the majority of mineral components in bentonite clay, and it primarily dominates the swelling and sorption characteristics of clay. The montmorillonite is further classified according to its exchangeable cation, and the most abundant types found in nature are the Na- and Ca-montmorillonites. In general, Na-montmorillonite has a higher swelling pressure than Ca-montmorillonite at moderate dry density (< ~1.5 $g \cdot cm^{-3}$), but it has been experimentally and theoretically reported that the Ca-montmorillonite can exhibit a greater swelling pressure than Na-montmorillonite at higher dry density [5-7]; most of commercial Ca-bentonite clays also provide sufficient swelling pressure to ensure the sealing and damping performances required for the engineered barrier system of deep geological repository (DGR) when manufactured in a form of compressed block with the dry density larger than 1.6 $g \cdot cm^{-3}$ [8]. Indeed, the Ca-bentonite clays are currently being considered as a candidate material for the construction of DGR in several countries; still, from a geochemical point of view, thermodynamic data on sorption reactions between the Ca-montmorillonite and dissolved nuclides of interest are lacking compared to that of Na-montmorillonite.

In this framework, we aimed to thoroughly analyze the chemical sorption properties of highly soluble fission products onto Ca-montmorillonite and establish a robust thermodynamic database. This study presents an overview of the utilization of TSM and experimental results for geochemical characterization of Ca-montmorillonite separated from the newly adopted reference bentonite (Bentonil-WRK) in the disposal performance demonstration R&D division of Korea Atomic Energy Research Institute (KAERI) by means of X-ray diffraction (XRD), Brunauer-Emmett-Teller (BET), cation exchange capacity (CEC) measurements, and controlled acid-base titration. Further, chemical sorption behaviors of monovalent cesium (Cs(I)) and divalent strontium (Sr(II)), which are the two major cationic fission products, onto the purified Ca-montmorillonite under aqueous conditions of S/L = 5 $g \cdot L^{-1}$, I = 0.01 M $CaCl_2$, pH = 4–9, $pCO_2 = 10^{-3.4}$ atm, and

T = 25°C were examined, and the resulting thermodynamic data and surface speciation were discussed.

2. Purification and Characterization of the Bentonil-WRK Montmorillonite

2.1 Physical and Chemical Treatments of the Bentonil-WRK Bentonite

Thus far, extensive experimental and modeling studies on the Thermal-Hydrological-Mechanical-Chemical-Biological (THMCB) properties of domestic KJ-I and KJ-II Ca-bentonites have been conducted in South Korea, but as the two clay resources are being depleted, the disposal performance demonstration R&D division of KAERI introduced a new reference Ca-bentonite clay called Bentonil-WRK (Clariant Korea) for HLW disposal research in 2021. The Bentonil-WRK bentonite has a montmorillonite content of ca. 75%, and the montmorillonite adsorbent was further separated and purified through the following procedure. Firstly, fine mineral particles were collected from the crushed Bentonil-WRK clay using a 200-mesh sieve and mixed with deionized water (Millipore, Milli-Q/RiOs) at a S/L ratio of 0.2 $kg \cdot L^{-1}$ subsequently. The mixture was mechanically stirred for 1 hour at a rotational speed of 600 rpm, and the particulate minerals were further dispersed for 30 minutes by applying 20 kHz ultrasonic pulse (15 seconds on/20 seconds off) with an intensity of 1,500 W (Sonics & Materials, VCX-1500). Then, the upper suspension was separated after 30 minutes of sedimentation and centrifuged at 5,000 rpm for 20 minutes (Thermo Scientific, Sorvall X1 Pro). The light-colored surficial fraction of precipitate was carefully collected and dried under ambient condition. The recovered powder sample was further reacted with pH 4 HCl solution (Sigma-Aldrich, ACS reagent) for 24 hours at a S/L ratio of 5 $g \cdot L^{-1}$ to remove trace amounts of carbonate impurities. Finally, the purified mineral sample was thoroughly washed with deionized water and lyophilized.

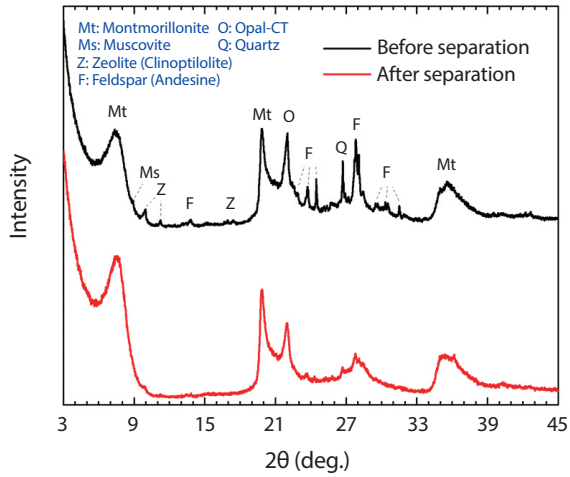

Fig. 1. XRD patterns of the raw Bentonil-WRK bentonite (black solid line) and purified montmorillonite (red solid line) samples.

2.2 XRD, BET, CEC, and Acid-Base Titration Analyses of the Purified Ca-type Bentonil-WRK Montmorillonite

XRD analysis provides qualitative and quantitative information on the mineral composition of analyte, and Fig. 1 shows the measured powder XRD patterns of both raw Bentonil-WRK bentonite and purified montmorillonite samples; the XRD spectra were recorded on the diffractometer (Bruker, Model D8 Advance) with a Cu Kα radiation source at 40 kV and 40 mA, and the measurement step size and acquisition time were 0.015° and 95.5 seconds per step, respectively. Signal assignment of the XRD patterns confirmed that feldspar, muscovite, opal-CT, quartz, and zeolite exist in the raw Bentonil-WRK clay as minor components, but those accessory minerals were effectively removed from the bentonite by performing the sequential physical and chemical treatments as described in section 2.1. Table 1 summarizes the results of quantitative Rietveld analysis on the XRD spectra obtained, and montmorillonite content in the purified clay sample was finally determined to be 95wt%.

In addition, specific surface areas of both raw Bentonil-WRK bentonite and purified montmorillonite were

Table 1. Mineral composition of the Bentonil-WRK bentonite and purified montmorillonite samples analyzed by the Rietveld method

Constituent minerals	Quantitative composition (wt%)	
	Bentonil-WRK bentonite	Purified montmorillonite
Montmorillonite	75	95
Feldspar	9	<1
Muscovite	6	2
Quartz	2	1
Opal-CT	4	2
Zeolite	4	<1

Table 2. CEC measurement of the Bentonil-WRK bentonite and purified montmorillonite samples

Exchangeable cations	Eluted concentrations of cations (meq/100 g)	
	Bentonil-WRK bentonite	Purified montmorillonite
Na	0.6	4.8
K	0.8	1.0
Ca	61.7	75.6
Mg	14.0	12.8
Sum	77.1	94.2

measured based on the BET theory. The mineral analytes were priorly degassed at 90°C for 18 hours, and multipoint BET analysis was conducted using a N_2 adsorption analyzer (Micromeritics, ASAP2010) subsequently. The resulting values were 59.1 and 74.4 $m^2 \cdot g^{-1}$ for raw and purified analytes, respectively; such increase in specific surface area after the physical and chemical treatments signifies an increase in montmorillonite content in the purified clay as well, and it proportionally corresponds to the Rietveld analysis of XRD spectra.

In the unit crystal structure of montmorillonite, two tetrahedral sheets of silica sandwich an octahedral sheet of alumina, and replacement of Al(III) with Mg(II) (i.e., isomorphic substitution) leads to a formation of permanent negative charges in the 2:1 T-O-T structure. Accordingly, cationic species are driven to sorption sites in the interlayer space (X) of montmorillonite to compensate electrostatic charge, which eventually makes the mineral has unique swelling and ion-exchange behaviors in an aqueous environment. CEC, which is defined as the total quantity of positive charges that can be exchanged on the negatively charged sites of clay mineral, is a major geochemical factor describing the chemical sorption properties of montmorillonite, and hence CEC of the purified Bentonil-WRK sample was assessed as well. Specifically, 0.1, 0.15, and 0.2 g of the purified montmorillonite samples were mixed with 100 mL of 0.5 M $CsNO_3$ (Sigma-Aldrich, 99%) neutral aqueous solutions, and the mixtures were stirred for 7 days with a rotational speed of 150 rpm at 25°C; Cs^+ has a stronger exchange affinity than the most of naturally occurring cations (e.g., Ca^{2+}, Mg^{2+}, Na^+, K^+, and etc.), and hence it was selected as an index cation in this study. After the reaction, supernatants were centrifuged at 5,000 rpm for 5 minutes and additionally filtered with PTFE membrane (Whatman) having a pore size of 200 nm. The eluted total concentrations of Ca^{2+}, Mg^{2+}, Na^+, K^+ were determined by means of inductively coupled plasma-optical emission spectroscopy (ICP-OES, Perkin Elmer, Optima 8300). As summarized in Table 2, it was confirmed that a predominant exchangeable cation in the purified Bentonil-WRK montmorillonite is Ca^{2+}, and

corresponding average CEC value was 94.2 meq/100 g; a proportional increase in CEC of the purified montmorillonite compared to that of raw bentonite confirms the appropriateness of physical and chemical treatments again.

In an aqueous medium, exchangeable cations of montmorillonite can be additionally replaced by hydrogen ions depending on the solution pH, and the external surface hydroxyl groups of clay also undergo pH-dependent protonation and deprotonation reactions. Therefore, it is essential to investigate such chemical interactions of hydrogen ions with montmorillonite to develop a robust thermodynamic sorption database for various radionuclides, and the corresponding reaction constants should be taken into account as they simultaneously compete for the limited sorption sites of montmorillonite. Accordingly, Ca^{2+}-H^{+} exchange and relevant protonation/deprotonation constants of the purified montmorillonite were further assessed by conducting the controlled continuous acid-base titration experiments and diffuse double layer model (DDLM) [9]-based geochemical modeling in the present work; considering the structural properties of 2:1 clay mineral, we simply assumed that the edge hydroxyl functionalities of montmorillonite are composed of amphoteric aluminol ([≡AlOH]) and monoprotic silanol ([≡SiOH]) groups. All sample preparation and experiment for acid-base titration were carried out in an Ar-filled glovebox system (KOREA KIYON, KK-011AS) to exclude the influence of atmospheric carbon dioxide (CO_2); it was confirmed that CO_2 level in the glovebox system utilized was maintained below 1 ppm during the entire processes. The homoionic Ca-montmorillonite suspension was prepared by saturating the purified mineral sample with 0.1 M $CaCl_2$ solution (Sigma-Aldrich, > 99%) at a S/L ratio of 2 $g \cdot L^{-1}$ for 7 days, and the Ca-montmorillonite suspension was thoroughly washed and lyophilized. Subsequently, the Ca-montmorillonite was re-dispersed in aqueous solutions having I = 0.01, 0.05, 0.1 M $CaCl_2$ at a S/L ratio of 5 $g \cdot L^{-1}$. The Ca-montmorillonite suspensions were firstly acidified to pH ca. 4 by adding a standardized 0.0225 M HCl solution (Sigma-Aldrich, ACS reagent), and they were gradually basified using a standardized 0.0051 M $CaOH_2$ titrant (Sigma-Aldrich, 99.995 %) until the pH values of supernatants reached ca. 9. During the titration, temperature of clay suspensions was maintained within the range of 25 ± 2℃, and the stepwise pH changes were measured using a glass combination electrode (Orion, 8107BN) and a potable pH meter (Orion, A326) while the suspensions were kept moderately stirred. The electrode potentials were recorded when the reading values reached a stability of ±0.1 mV per 20 seconds, and it generally took 3–4 minutes for each titration step. The uncertainty of measured pH values was conservatively assigned to be ±0.05, which is a typical reproducibility of the utilized pH electrode observed. Further, actual molar proton concentrations of supernatants were corrected from the measured pH values based on a simple empirical method as described elsewhere [10]. From the resulting acid-base titration curves (i.e., change in pH of the suspensions versus volume of acid/base titrants added), the net surface proton excess (ΔQ) of Ca-montmorillonite at each titration point can be calculated as described in Equation (1). In Equation (1), C_a and C_b denotes molar concentrations of acid and base titrants added, $[H^{+}]$ and $[OH^{-}]$ are molar concentrations of hydrogen and hydroxide ions corrected from the measured pH, and M indicates the S/L ratio of suspension analyte, respectively; ionic strength dependence of the ionization constant of water (K_w) was calculated and reflected using the Davies equation [11]. Site densities of the reactive hydroxyl functionalities and thermodynamic constants of relevant surfaces reactions (see Equation (2)–(5)) were eventually refined from the experimental ΔQ data using a geochemical modeling code PHREEQC [12] coupled with parameter estimation tool PEST [13]; thermodynamic activities of exchange and surface species were considered to be equal to their equivalent and mole fraction for each site, respectively. The Davies equation was adopted to correct the activity coefficients of dissolved species as well, and Table 3 summarizes the optimization results. All statistical uncertainties provided in Table 3 correspond to a 95% confidence level, and Fig. 2 displays the experimental ΔQ values (open

Table 3. Acid-base reaction parameters of the purified Ca-type Bentonil-WRK montmorillonite

Surface reaction	log K
$X_2Ca + 2H^+ \rightleftharpoons 2XH + Ca^{2+}$	3.38 ± 0.06
$\equiv AlOH + H^+ \rightleftharpoons \equiv AlOH_2^+$	8.35 ± 0.24
$\equiv AlOH \rightleftharpoons \equiv AlO^- + H^+$	−9.59 ± 0.28
$\equiv SiOH \rightleftharpoons \equiv SiO^- + H^+$	−7.65 ± 0.09
Surface site	**Total site density**
X	94.2 meq/100 g*
≡AlOH	$(4.94 \pm 0.12)\times10^{-5}$ mol·g^{-1}
≡SiOH	$(7.42 \pm 0.87)\times10^{-5}$ mol·g^{-1}

* adopted value from the CEC measurement

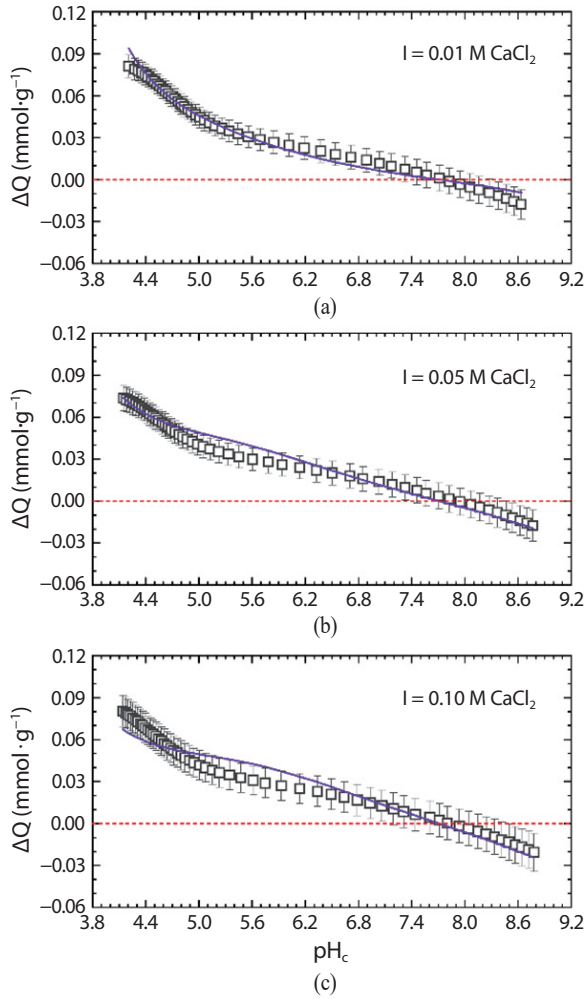

Fig. 2. Experimentally evaluated net surface proton excess of the purified Ca-type Bentonil-WRK montmorillonite as a function of pH_c (open square) and their modeling results (solid line) at different ionic strengths: (a) 0.01 M $CaCl_2$; (b) 0.05 M $CaCl_2$; (c) 0.10 M $CaCl_2$.

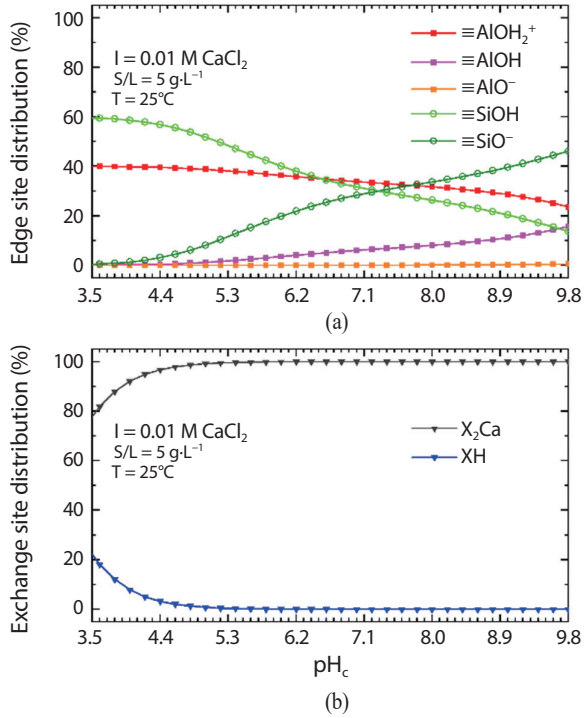

Fig. 3. Calculated surface species distribution of the Ca-type Bentonil-WRK montmorillonite at I = 0.01 M $CaCl_2$, S/L = 5 g·L^{-1}, and T = 25°C: (a) edge hydroxyl sites; (b) interlayer exchange sites.

square) of purified Ca-type Bentonil-WRK montmorillonite at different ionic strengths and their comparisons with the DDLM-based computed data (solid line); the optimized acid-base reaction parameters reproduce the experimental data fairly well under the studied aqueous conditions (pH = 4–9, I = 0.01–0.1 M $CaCl_2$, S/L = 5 g·L^{-1}, and T = 25 ± 2°C), and they were successfully used as primary input data for thermodynamic sorption modeling of Cs(I) and Sr(II) onto the Ca-montmorillonite. A general view on the pH-dependent distribution of edge hydroxyl and interlayer exchanges sites in the purified Ca-montmorillonite is presented in Fig. 3, clearly showing the active acid-dissociation behaviors of both aluminol and silanol groups in the pH range of 4–10 and the predominance of Ca-exchanged interlayer sites at pH > 5.

$$\Delta Q = ([XH] + [\equiv AlOH_2^+] - [\equiv AlO^-] - [\equiv SiO^-]) \times M^{-1} = (C_a - C_b - [H^+] + [OH^-]) \times M^{-1} \quad (1)$$

$$X_2Ca + 2H^+ \rightleftharpoons 2XH + Ca^{2+} \quad (2)$$

$$\equiv AlOH + H^+ \rightleftharpoons \equiv AlOH_2^+ \quad (3)$$

$$\equiv AlOH \rightleftharpoons \equiv AlO^- + H^+ \quad (4)$$

$$\equiv SiOH \rightleftharpoons \equiv SiO^- + H^+ \quad (5)$$

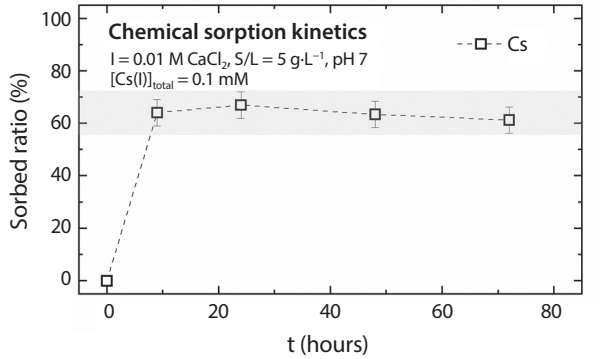

Fig. 4. Chemical sorption kinetics of Cs(I) onto the purified Ca-type Bentonil-WRK montmorillonite at I = 0.01 M $CaCl_2$, S/L = 5 g·L^{-1}, pH 7, and T = 25 ± 1°C.

3. Sorption Behaviors of Cs(I) and Sr(II) Onto the Purified Ca-type Bentonil-WRK Montmorillonite

3.1 Batch Sorption Experiment and Thermodynamic Modeling for Cs(I)

Cesium, which is one of the major fission products included in HLW, only has a stable oxidation state of +1 in an aqueous solution, and the high solubility of Cs(I) facilitates its rapid transport in the natural water systems by advection; understanding the chemical sorption mechanisms of Cs(I) onto montmorillonite and evaluating the relevant thermodynamic reaction constants are essential to accurately predict the retention and long-term migration behaviors of Cs(I) in a DGR. In the present work, totally 55 batch samples (S/L = 5 g·L^{-1} and pH 4–9), classified into 4 groups according to their total concentration of Cs(I) and ionic strength conditions, were prepared to evaluate chemical sorption of Cs(I) onto the purified Ca-type Bentonil-WRK montmorillonite (group 1: $[Cs(I)]_{total}$ = 0.1 mM and I = 0.01 M $CaCl_2$, group 2: $[Cs(I)]_{total}$ = 0.2 mM and I = 0.01 M $CaCl_2$, group 3: $[Cs(I)]_{total}$ = 0.4 mM and I = 0.01 M $CaCl_2$, group 4: $[Cs(I)]_{total}$ = 0.4 mM and I = 0.03 M $CaCl_2$). Specifically, the precisely weighed homoionic Ca-montmorillonite samples were pretreated with $CaCl_2$ solutions for 3 days with constant end-over-end shaking where the pH values of supernatants were adjusted with concentrated HCl and $CaOH_2$ solutions. After the pretreatment, appropriated amounts of CsCl (Sigma-Aldrich, 99.9%) stock solutions were added to the suspensions, and the sorption samples were allowed to equilibrate for another 3 days in a benchtop incubated shaker (Lab Companion, IST-4075R) under ambient conditions at 25 ± 1°C, followed by separation of supernatant from the solid adsorbent by centrifugation at 5,000 rpm for 10 minutes. Final pH values of the supernatants were recorded and corrected as described in section 2.2, and dissolved concentrations of Cs(I) and Al(III) in the solutions were determined by inductively coupled plasma-mass spectrometry (Perkin Elmer, NexION 350X); the quantified Al(III) concentrations were below a detection limit (5 ppb) for the all samples, indicating that the solid-liquid separation process was effective. Fig. 4 shows the evaluated sorption kinetics of Cs(I) onto the purified Ca-type Bentonil-WRK montmorillonite at pH 7, indicating that the chemical sorption reaction generally reached an equilibrium state within 24 hours.

Fig. 5 presents Kd values calculated from the entire batch sorption data, and it shows the gradual enhancement of Cs(I) sorption onto the Ca-montmorillonite with increasing pH. Under the acidic conditions, it is explained by a competition between H^+ and Cs^+ cations for the interlayer sites, whereas this tendency also implies that the surface complexation between Cs^+ and edge hydroxyl sites of montmorillonite additionally occurs in the basic pH region since the precipitation of ~10^{-4} M dissolved Cs(I) can be

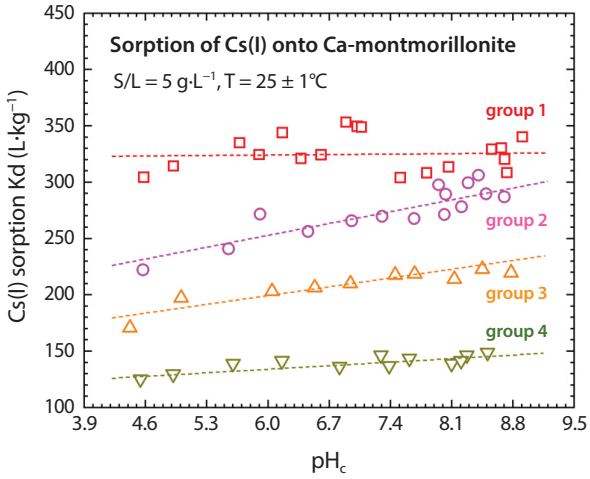

Fig. 5. Resulting Kd values of Cs(I) for the purified Ca-type Bentonil-WRK montmorillonite at different pH, I, and $[Cs]_{total}$ conditions.

Table 4. Thermodynamic sorption constants for surface reactions of Cs(I) and Sr(II) onto the purified Ca-type Bentonil-WRK montmorillonite

Surface reaction	log K
$X_2Ca + 2Cs^+ \rightleftarrows 2XCs + Ca^{2+}$	2.32 ± 0.04
$X_2Ca + Sr^{2+} \rightleftarrows X_2Sr + Ca^{2+}$	−0.05 ± 0.02
$\equiv SiOH + Cs^+ \rightleftarrows \equiv SiOCs + H^+$	−5.62 ± 0.38
$\equiv SiOH + Sr^{2+} \rightleftarrows \equiv SiOSr^+ + H^+$	−6.85 ± 0.41

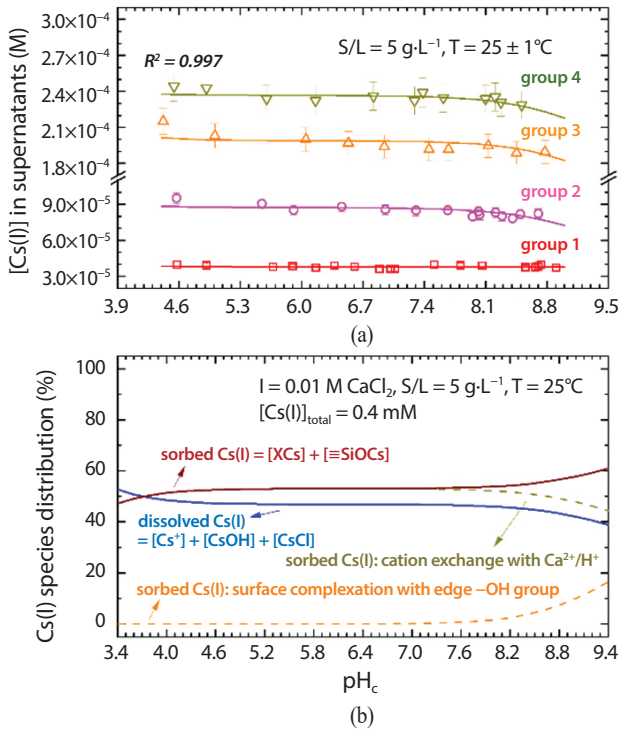

Fig. 6. (a) Experimentally assessed [Cs(I)] in the supernatants of batch samples (open symbol) and their DDLM-based modeling results (solid line); (b) species distribution of Cs(I) adsorbed onto the purified Ca-type Bentonil-WRK montmorillonite at I = 0.01 M $CaCl_2$, S/L = 5 g·L^{-1}, T = 25°C, and $[Cs]_{total}$ = 0.4 mM.

generally excluded in the Ca-H-Cl-CO_3-OH aqueous system. In order to estimate the corresponding surface reaction constants from the experimental sorption data, a combination of PHREEQC and PEST codes was utilized again to perform the DDLM-based geochemical calculation. Firstly, along with the Ca^{2+}-Cs^+ exchange reaction at the interlayer sites (see Equation (6)), the surface complexations of Cs^+ with both aluminol (see Equation (7)) and silanol (see Equation (8)) functionalities were considered in the inverse modeling. However, it was identified that silanol group is more likely to be involved in the surface complexation than aluminol group through a parametric reaction sensitivity analysis, and that the experimental sorption data can be satisfactorily fitted even though only the silanol complexation is taken into account in the thermodynamic modeling in conjunction with the cation exchange mechanism. Therefore, by adopting the principle of Ockham's Razor, surface reactions (6) and (8) were reflected in the geochemical calculation, and the refined constants are summarized in Table 4; such surface reaction model is comparable with that used in the previous study to describe Cs(I) sorption onto MX-80 bentonite in a synthetic groundwater medium [14], and the stability constants of aqueous CsCl(aq) and CsOH(aq) complexes, required for the accurate geochemical modeling, were adopted from the ThermoChimie DB v12a [15]. All uncertainties provided in Table 4 correspond to a 95% confidence level, and Fig. 6(a) displays an acceptable accordance between the experimentally assessed [Cs(I)] remaining in the sorption supernatants (open symbol) and their DDLM-based computed data (solid line). Finally, Fig. 6(b) illustrates the distribution of surface Cs(I) species adsorbed onto the purified Ca-montmorillonite, which

demonstrates the predominance of cation exchange-driven sorption characteristic of Cs(I) under the acidic-neutral pH conditions and additional formation of the ≡SiOCs surface complex at pH > 8; the thermodynamic reaction model and surface speciation of Cs(I) onto Ca-montmorillonite scrutinized in the present work are fairly consistent with the previously reported pH-dependent sorption behavior of Cs(I) onto the Na-montmorillonite [14, 16] as well.

$$X_2Ca + 2Cs^+ \rightleftharpoons 2XCs + Ca^{2+} \quad (6)$$

$$\equiv AlOH + Cs^+ \rightleftharpoons \equiv AlOCs + H^+ \quad (7)$$

$$\equiv SiOH + Cs^+ \rightleftharpoons \equiv SiOCs + H^+ \quad (8)$$

3.2 Batch Sorption Experiment and Thermodynamic Modeling for Sr(II)

Strontium exists in a +2 oxidation state in an aqueous medium, and it generally has a solubility in the range of 10^{-5}~10^{-2} M under the natural water environments, which is still higher than most of other constituent nuclides in HLW (e.g., actinides, lanthanides, etc.); investigating the geochemical interactions between Sr(II) and montmorillonite is important from a viewpoint of enhancing the reliability in a performance assessment of DGR as well. Similar to the Cs(I) sorption experiment, 57 batch samples (S/L = 5 g·L^{-1} and pH 4–9) were prepared in this study to evaluate sorption behavior of Sr(II) onto the purified Ca-type Bentonil-WRK montmorillonite, where the experimental sets were classified into 4 groups according to the total concentration of Sr(II) and ionic strength conditions (group 1: $[Sr(II)]_{total}$ = 0.05 mM and I = 0.01 M $CaCl_2$, group 2: $[Sr(II)]_{total}$ = 0.1 mM and I = 0.01 M $CaCl_2$, group 3: $[Sr(II)]_{total}$ = 0.2 mM and I = 0.01 M $CaCl_2$, group 4: $[Sr(II)]_{total}$ = 0.2 mM and I = 0.03 M $CaCl_2$). The Sr(II) stock solutions were made by dissolving powdered $SrCl_2 \cdot 6H_2O$ (Sigma-Aldrich, 99%) in deionized water, and the rest experimental methods used for the pretreatment of purified Bentonil-WRK montmorillonite,

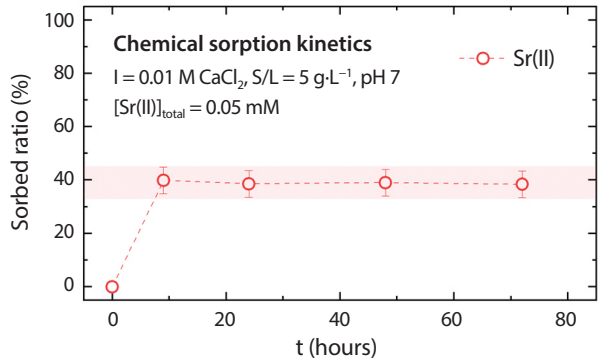

Fig. 7. Chemical sorption kinetics of Sr(II) onto the purified Ca-type Bentonil-WRK montmorillonite at I = 0.01 M $CaCl_2$, S/L = 5 g·L^{-1}, pH 7, and T = 25 ± 1°C.

evaluation on chemical sorption of Sr(II), and data analysis were identical to those of the Cs(I) experiment detailed in section 3.1. Fig. 7 shows the resulting sorption kinetics of Sr(II) onto the Ca-montmorillonite at pH 7, which signifies that the Sr(II) sorption reaction reached a chemical equilibrium within 24 hours in general.

The assessed Kd values of Sr(II) for Ca-montmorillonite are depicted in Fig. 8, and a slight but gradual increase in the Kd values were observed with increasing pH, as similar to the Cs(I) sorption behavior. Such chemical trend can also be explained by the competitive cation exchange of H^+ with Sr^{2+} at the interlayer of montmorillonite under acidic conditions and the additional formation of surface Sr(II) complex with edge hydroxyl sites of montmorillonite under neutral-basic conditions; precipitation of $Sr(OH)_2$ or $SrCO_3$ in the studied aqueous system can be ruled out according to the geochemical calculation as well. By performing a parametric reaction analysis using the PHREEQC and PEST codes, the surface complexation of Sr^{2+} with aluminol functionality of montmorillonite (see Equation (10)) was excluded from the subsequent inverse modeling of sorption data; in other words, only surface reactions of Sr^{2+} at the interlayer site (see Equation (9)) and edge silanol group (see Equation (11)) of montmorillonite were considered. The stability constants of aqueous $SrOH^+$, $SrCl^+$, $SrHCO_3^+$, and $SrCO_3$(aq) species were

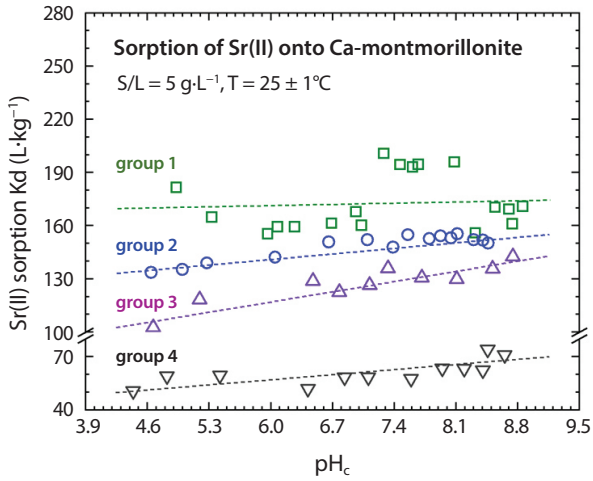

Fig. 8. Assessed Kd values of Sr(II) for the homoionic Ca-montmorillonite at different pH, I, and $[Sr]_{total}$ conditions.

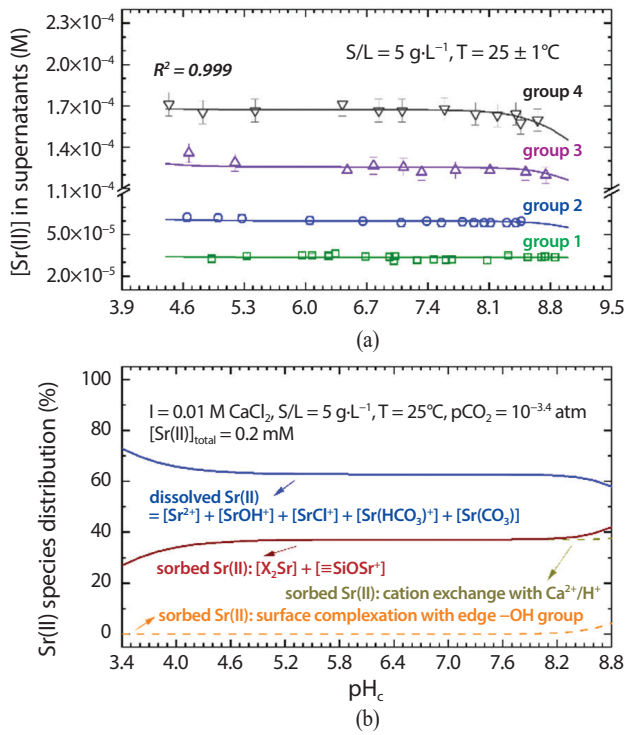

Fig. 9. (a) Resulting dissolved [Sr(II)] in the supernatants of batch samples (open symbol) and their DDLM-based computed data (solid line); (b) Sr(II) species distribution adsorbed onto the purified Ca-type Bentonil-WRK montmorillonite at I = 0.01 M $CaCl_2$, S/L = 5 g·L^{-1}, T = 25°C, $pCO_2 = 10^{-3.4}$ atm, and $[Sr]_{total}$ = 0.2 mM.

taken from the ThermoChimie DB v12a [15] and reflected in the geochemical calculation. The DDLM-based refined reaction constants are provided in Table 4 as well, and Fig. 9(a) shows the good agreement between the experimental Sr(II) sorption data (open symbol) and modeling result (solid line). Finally, Fig. 9(b) displays the distribution of surface Sr(II) species adsorbed onto the purified Ca-type Bentonil-WRK montmorillonite under aqueous conditions of I = 0.01 M $CaCl_2$, S/L = 5 g·L^{-1}, T = 25°C, $pCO_2 = 10^{-3.4}$ atm, and $[Sr]_{total}$ = 0.2 mM, representing that the Sr(II) sorption behavior is primarily governed by the cation exchange mechanism over the entire pH range, whereas the formation of $\equiv SiOSr^+$ species under basic conditions is thermodynamically weaker than that of Cs(I)-silanol surface complex; such geochemical understanding on surface reaction of Sr(II) with Ca-montmorillonite also agrees well with the previously reported chemical sorption characteristics of Sr(II) onto Na-smectite clays [17, 18].

$$X_2Ca + Sr^{2+} \rightleftharpoons X_2Sr + Ca^{2+} \quad (9)$$

$$\equiv AlOH + Sr^{2+} \rightleftharpoons \equiv AlOSr^+ + H^+ \quad (10)$$

$$\equiv SiOH + Sr^{2+} \rightleftharpoons \equiv SiOSr^+ + H^+ \quad (11)$$

4. Concluding Remark

Adsorption characteristics of the radionuclides contained in HLW onto montmorillonite should be explicitly investigated to reliably assess the radionuclide retention capacity of engineered barriers in a DGR. Utilization of TSM in the performance assessment of DGR generally improves the confidence in demonstrating and evaluating the chemical sorption phenomena under a wide range of aqueous conditions, and hence it is ultimately expected to reduce uncertainty and enhance predictability in assessing the long-term migration of radionuclides under the DGD environment. In this framework, we aimed to scrutinize the chemical sorption mechanisms of fission products onto Ca-montmorillonite and establish a robust thermodynamic database. As a first step, this study presents the purification and geochemical

characterization of Ca-montmorillonite separated from the newly adopted Bentonil-WRK clay in the disposal performance demonstration R&D division of KAERI, and its sorption thermodynamics with Cs(I) and Sr(II), which are the two major cationic fission products having relatively high solubility, onto the purified Ca-montmorillonite under ambient conditions were investigated by the DDLM-based TSM; the established surface reaction models and associated thermodynamic constants successfully represented the sorption characteristics of Cs(I) and Sr(II) over the studied aqueous conditions, where logarithms of thermodynamic constants for the surface reactions of 1) $X_2Ca + 2Cs^+ \rightleftharpoons 2XCs + Ca^{2+}$, 2) $X_2Ca + Sr^{2+} \rightleftharpoons X_2Sr + Ca^{2+}$, 3) $\equiv SiOH + Cs^+ \rightleftharpoons \equiv SiOCs + H^+$, and 4) $\equiv SiOH + Sr^{2+} \rightleftharpoons \equiv SiOSr^+ + H^+$ were determined to be 2.32 ± 0.04, −0.05 ± 0.02, −5.62 ± 0.38, and −6.85 ± 0.41, respectively. The predominant surface reaction mechanism of both Cs(I) and Sr(II) onto Ca-montmorillonite was confirmed to be cation exchange at the interlayer site, while surface complexation of the fission products with edge silanol group was additionally identified as responsible for the slight enhancement of their sorption at pH > 8. Further experimental and modeling works should be devoted to expanding the target adsorbate for sorption study of the purified Ca-type Bentonil-WRK montmorillonite (i.e., anionic fission products, activation products, and actinides), and to exploring the sorption thermodynamics under the wider geochemical conditions, such as higher temperature, ionic strength, and pH as well.

Conflict of Interest

No potential conflict of interest relevant to this article was reported.

Acknowledgements

This study was supported by the Institute for Korea Spent Nuclear Fuel (iKSNF) and National Research Foundation of Korea (NRF) grant funded by the Korean Ministry of Science and ICT (Grant code: 2021M2E1A1085202).

REFERENCES

[1] S. Choi, H.S. Im, J.Y. Goo, H. Lee, J.W. Kim, G.Y. Kim, D.K. Cho, and J.S. Kwon. Analysis of the POSIVA FEPs for KBS-3V Disposal System: I. Multiple-barrier Repository Subsystem, Korea Atomic Energy Research Institute Report, KAERI/AR-1376/2021 (2021).

[2] V. Brendler, A. Vahle, T. Arnold, G. Bernhard, and T. Fanghänel, "RES^{3}T-Rossendorf Expert System for Surface and Sorption Thermodynamics", J. Contam. Hydrol., 61 (1-4), 281-291 (2003).

[3] M. Ochs, J.A. Davis, M. Olin, T.E. Payne, C.J. Tweed, M.M. Askarieh, and S. Altmann, "Use of Thermodynamic Sorption Models to Derive Radionuclide K_d Values for Performance Assessment: Selected Results and Recommendations of the NEA Sorption Project", Radiochim. Acta, 94(9-11), 779-785 (2006).

[4] T.E. Payne, V. Brendler, M. Ochs, B. Baeyens, P.L. Brown, J.A. Davis, C. Ekberg, D.A. Kulik, J. Lutzenkirchen, T. Missana, Y. Tachi, L.R. Van Loon, and S. Altmann, "Guidelines for Thermodynamic Sorption Modelling in the Context of Radioactive Waste Disposal", Environ. Model. Softw., 42, 143-156 (2013).

[5] O. Karnland, S. Olsson, and U. Nilsson. Mineralogy and Sealing Properties of Various Bentonites and Smectite-rich Clay Materials, Swedish Nuclear Fuel and Waste Management Company Technical Report, TR-06-30 (2006).

[6] L. Sun, J.T. Hirvi, T. Schatz, S. Kasa, and T.A. Pakkanen, "Estimation of Montmorillonite Swelling Pressure: A Molecular Dynamics Approach", J. Phys. Chem. C, 119(34), 19863-19868 (2015).

[7] B. Akinwunmi, J.T. Hirvi, S. Kasa, and T.A. Pakkanen, "Swelling Pressure of Na- and Ca-Montmorillonites in

Saline Environments: A Molecular Dynamics Study", Chem. Phys., 528, 110511 (2020).

[8] M. Kim, J. Lee, S. Yoon, S. Choi, M. Kong, and J.S. Kim. Comparison and Analysis of Physical Properties Database for Buffer Material Candidates, Korea Atomic Energy Research Institute Technical Report, KAERI/TR-9795/2023 (2023).

[9] S. Goldberg, L.J. Criscenti, D.R. Turner, J.A. Davis, and K.J. Cantrell, "Adsorption-Desorption Processes in Subsurface Reactive Transport Modeling", Vadose Zone J., 6(3), 407-435 (2007).

[10] S. Choi and J.I. Yun, "Spectrophotometric Study of the Uranyl Monobenzoate Complex at Moderate Ionic Strength", Polyhedron, 161, 120-125 (2019).

[11] I. Grenthe, F. Mompean, K. Spahiu, and H. Wanner, TDB-2 Guidelines for the Extrapolation to Zero Ionic Strength, OECD Nuclear Energy Agency, Issy-les-Moulineaux, France (2013).

[12] D.L. Parkhurst and C.A.J. Appelo, Description of Input and Examples for PHREEQC Version 3–A Computer Program for Speciation, Batch-Reaction, One-Dimensional Transport, and Inverse Geochemical Calculations, U.S. Geological Survey, Reston, VA (2013).

[13] J. Doherty, Calibration and Uncertainty Analysis for Complex Environmental Models, Watermark Numerical Computing, Brisbane, Australia (2015).

[14] C. Hurel, N. Marmier, F. Sévy, E. Giffaut, A.C.M. Bourg, and F. Fromage, "Sorption Behaviour of Caesium on a Bentonite Sample", Radiochim. Acta, 90(9-11), 695-698 (2002).

[15] E. Giffaut, M. Grivé, Ph. Blanc, Ph. Vieillard, E. Colàs, H. Gailhanou, S. Gaboreau, N. Marty, B. Madé, and L. Duro, "Andra Thermodynamic Database for Performance Assessment: ThermoChimie", Appl. Geochem., 49, 225-236 (2014).

[16] C. Hurel, N. Marmier, A. Bourg, and F. Fromage, "Sorption of Cs and Rb on Purified and Crude MX-80 Bentonite in Various Electrolytes", J. Radioanal. Nucl. Chem., 279(1), 113-119 (2009).

[17] T. Missana, M. Garcia-Gutierrez, and U. Alonso, "Sorption of Strontium Onto Illite/Smectite Mixed Clays", Phys. Chem. Earth, Parts A/B/C, 33(1), S156-S162 (2008).

[18] Y. Sugiura, T. Ishidera, and Y. Tachi, "Surface Complexation of Ca and Competitive Sorption of Divalent Cations on Montmorillonite Under Alkaline Conditions", Appl. Clay Sci., 200, 105910 (2021).